ENDOR and Special Triple Resonance Studies of Chlorophyll Cation Radicals in Photosystem 2†

Stephen E. J. Rigby,‡ Jonathan H. A. Nugent,*,‡ and Patrick J. O'Malley§

Department of Biology, Darwin Building, University College London, Gower Street, London, WC1E 6BT, U.K., and Department of Chemistry, UMIST, P.O. Box 88, Manchester, M60 1QD, U.K.

Received March 22, 1994; Revised Manuscript Received June 14, 1994®

ABSTRACT: Electron nuclear double resonance (ENDOR) and special triple (ST) resonance spectroscopies have been used to study the cation radicals of the primary donor, P680, and two secondary donor chlorophylls (Chl) in photosystem 2 (PS2). Two different preparations were employed, Tris-washed PS2 membranes and PS2 reaction centers (D1–D2–I–Cytb_{559} complex). One secondary donor Chl *a* cation radical, Chl1$^{\bullet+}$, was generated in the Tris-washed preparation, while the P680$^{\bullet+}$ radical cation and a further Chl *a* cation radical, Chl2$^{\bullet+}$, were produced in the reaction center preparation. The ENDOR spectrum of the primary donor radical cation of photosystem 1 (P700$^{\bullet+}$) is also presented for comparison. Hyperfine coupling constants for methyl groups have been measured for all three PS2 radical species and assigned by comparison with previously published spectra of Chl *a* radicals *in vitro*. Electron spin densities were calculated from these hyperfine couplings. Comparison of ENDOR spectral features with those of Chla$^{\bullet+}$ *in vitro* indicates similar values for Chl1$^{\bullet+}$ and Chl2$^{\bullet+}$ radicals but an apparent reduction in unpaired electron spin density for P680$^{\bullet+}$. It has been proposed from the more detailed studies of purple bacterial reaction centers that such a reduction in spin density can be interpreted as a delocalization over two Chl *a* molecules. Our calculations therefore suggest that P680$^{\bullet+}$ is a weakly coupled chlorophyll pair with 82% of the unpaired electron spin located on one chlorophyll of the pair at 15 K. Environmental or geometrical changes to the chlorin ring structure to give a novel monomeric primary donor are also possible. The secondary donor Chl *a*'s are both monomeric, the species in the reaction center preparation possibly lacking amino acid coordination at the magnesium ion. These data are discussed in the light of previous studies of P680 and oxidized chlorophyll species in PS2 using other techniques.

The primary process of energy transduction in photosystem 2 (PS2)[1] comprises (Evans & Nugent 1993) absorption of light quanta by the light-harvesting system leading to formation of electronically excited states; the trapping of this excitation energy at a special Chl *a* site called P680 (pigment absorbing at 680 nm); ejection of an electron from the excited singlet state of the primary donor P680, forming the radical cation P680$^{\bullet+}$, and acceptance of this electron by a pheophytin *a* (I); and stabilization of this charge-separated state by electron transfer from I$^{\bullet-}$ to a plastoquinone (Q_A) iron complex. This sequence of events and the cofactors involved are very similar to those occurring in the photosynthetic reaction centers (RCs) of purple sulfur bacteria such as *Rhodobacter sphaeroides* and *Rhodopseudomonas viridis* [for reviews of bacterial RC struture and function, see Deisenhofer and Norris (1993)]. The L and M subunits of the bacterial RC also show sequence homology with the D1 and D2 proteins (*psbA* and *psbD* gene products), respectively, which bear the redox-active cofactors of PS2 (Svensson et al., 1990; Ruffle et al., 1992). Since the three-dimensional structure of the bacterial RC has been determined to high resolution using X-ray crystallography (Deisenhofer et al., 1985; Allen et al., 1986), it is possible to model the structure of the PS2 D1–D2 reaction center complex using the bacterial RC as a template (Svensson et al., 1990; Ruffle et al., 1992). While such models may be correct in gross structure, fine structural details may not be conserved between bacterial and PS2 RCs.

One such detail concerns the structure of the primary donor. The primary donor of *R. sphaeroides* RC, P870, is a closely spaced pair of bacteriochlorophyll *a* molecules with a midpoint redox potential of *circa* 490 mV, some 200 mV lower than that of bacteriochlorophyll *a in vitro* (Blankenship & Prince, 1985). A similar situation pertains to the primary donor of *Rps. viridis*, P960, which is a bacteriochlorophyll *b* pair. P680, however, exhibits a redox potential of *circa* 1.1 V compared to *circa* 830 mV for Chl *a in vitro* (Blankenship & Prince, 1985). Therefore the formation of P680 has an effect on its constituent Chl *a* molecule(s) fundamentally different from that exhibited by the bacterial primary donor. The causes of such differences in behavior may be delineated using spectroscopic approaches.

Electron paramagnetic resonance (EPR) spectroscopy has been used to characterize radical ion and triplet states of redox-active cofactors in both prokaryotic and eukaryotic photosynthetic systems. EPR spectra of the radical ion states of the primary donor, the pheophytin acceptor, and the iron quinone complex have been obtained for both the bacterial RCs (Hoff, 1993) and PS2 (Miller & Brudvig, 1991; Evans & Nugent, 1993). Electron nuclear double resonance (ENDOR) and electron nuclear special triple resonance (special

† We acknowledge financial assistance from the U.K. Science and Engineering Research Council.

* Address correspondence to this author.

‡ University College London.

§ UMIST.

® Abstract published in *Advance ACS Abstracts,* August 1, 1994.

[1] Abbreviations: Chl, chlorophyll; Chl1, the secondary donor chlorophyll oxidized in Tris washed PS2; Chl2, the secondary donor chlorophyll of PS2 reaction centers; Chla$^{\bullet+}$, chlorophyll *a* radical cation in vitro; EPR, electron paramagnetic resonance; ENDOR, electron nuclear double resonance; PS1, photosystem 1; PS2, photosystem 2; P680, the primary donor chlorophyll(s) of PS2; P700, the primary donor chlorophyll(s) of PS1; P870, the primary donor of the *Rhodobacter sphaeroides* reaction center; P960, the primary donor of the *Rhodopseudomonas viridis* reaction center; RC; reaction center; ST, special electron nuclear triple resonance spectroscopy; Tris, tris(hydroxymethyl)aminomethane; ν_H, proton Larmor frequency.

0006-2960/94/0433-10043$04.50/0

triple, or ST) (Freed, 1969; Dinse et al., 1974; Möbius & Biehl, 1979; Kurreck et al., 1988) have extended studies of the bacterial system to the determination of individual hyperfine coupling constants (hfcs) in frozen solution (Feher et al., 1975, 1988; Norris et al., 1975; Lubitz et al., 1984; Lendzian et al., 1988) and, where possible, in liquid solution (Kurreck et al., 1988; Lendzian et al., 1992; Rautter et al., 1992) and single crystals (Lendzian et al., 1993). Such techniques provide information on values of the unpaired electron spin densities within the radical species, which can be interpreted structurally. ENDOR originally suggested that the primary donor in bacterial RCs was a bacteriochlorophyll dimer (Feher et al., 1975; Norris et al., 1975), a result subsequently confirmed by the determination of the RC structure. ENDOR has also been successfully applied to radicals formed in PS2, specifically the acceptor pheophytin $I^{\bullet-}$ (Lubitz et al., 1989) and the tyrosine radical $Y_D^{\bullet}$ (O'Malley et al., 1984; Chandrashekar et al., 1986; Rigby et al., 1994). However, no major study of the ENDOR spectra of Chl *a* cation radicals in PS2 has been reported.

Here we present an ENDOR and ST study of $P680^{\bullet+}$ and two presumptive monomeric Chl *a* radical cations of PS2. ENDOR spectra of the primary donor cation radical of PS1, $P700^{\bullet+}$, are presented for comparison. From this data we have developed models for the electron spin density distributions in these species. These provide indications of the structure and environment of the redox-active Chl *a* species of PS2.

MATERIALS AND METHODS

Chloroplast thylakoid membranes (12 mg of Chl/mL) and PS2 membranes (BBYs; Berthold et al., 1981; Chl *a*/Chl *b* ratio, 2.05–2.20:1) were prepared from market spinach (*Spinacea oleracea*) by the method of Ford and Evans (1983). The Tris-washed material (depleted of manganese and the three extrinsic lumenal proteins) was prepared from BBY particles by incubation in 1 M Tris-HCl, pH 8.8, on ice under room illumination for 1 h followed by centrifugation at 40000*g* for 30 min at 4 °C. Samples for spectroscopy were resuspended in 50 mM Tris-HCl, pH 8.8, 5 mM $MgCl_2$, 100 μM EGTA, and 0.3 M sucrose at 15–20 mg of Chl/mL.

PS2 reaction centers containing D1, D2, psbI gene product, and cytochrome b_{559} were prepared from the Tris-washed material using a procedure based on that of Nanba and Satoh (1987), as modified by Barber et al. (1987) and Demetriou (1990). Tris-washed PS2 was centrifuged at 40000*g* for 30 min at 4 °C, and the pellet was resuspended under low-light conditions in 50 mM Tris-HCl, pH 7.2, 4% (w/v) Triton X-100, and 1 mM *o*-phenanthroline at 1 mg of Chl/mL. This suspension was incubated on ice in the dark for 90 min with continuous gentle stirring. These solubilized complexes were then centrifuged at 40000*g* for 30 min at 4 °C, and the resulting supernatant was loaded onto a DEAE-Fractogel (Merck) column preequilibrated with 50 mM Tris-HCl, pH 7.2, 0.2% (w/v) Triton X-100, 30 mM sodium chloride (NaCl), and 1 mM *o*-phenanthroline. The column was washed with 20 column volumes of the same buffer and then developed with a stepwise salt gradient running from 30 to 120 mM NaCl in 50 mM Tris-HCl, pH 7.2, 4 mM dodecyl β-D-maltoside, and 1 mM *o*-phenanthroline. The reaction centers eluted in the 120 mM NaCl fraction and were concentrated to 50–70 μM using Minicon concentrators (Amicon) with a 15-kDa cutoff. Sucrose was added to a final concentration of 0.35 M before samples were prepared for spectroscopy. The long wavelength maximum of the reaction center absorption spectrum was at 676.2 nm.

Spinach PS1 particles were prepared as previously described (Williams-Smith et al., 1978) using Triton X-100. *Synechocystis* PS1 was prepared as in Biggins and Mathis (1988). Chromatophores of the purple bacteria *R. sphaeroides* and *Rps. viridis* were prepared as in Clayton and Clayton (1978).

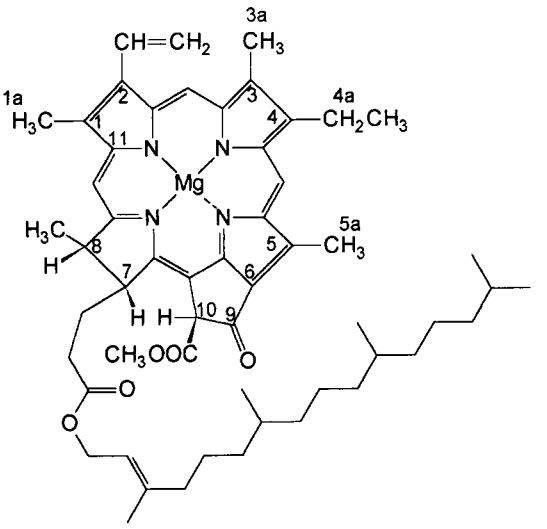

FIGURE 1: Structure and atom numbering scheme of chlorophyll *a*.

Sample volumes were 150–300 μL in 3-mm-i.d. quartz EPR tubes. The Chl *a* radical was generated in Tris-washed PS2 by illumination in liquid nitrogen (77 K) with an unfiltered 300-W white light source, as was the $P700^{\bullet+}$ radical in PS1. Radicals were produced in reaction center samples by illumination in the ENDOR cavity at cryogenic temperatures using a 150-W white light source via a 3-mm-diameter optical fiber.

ENDOR, ST, and EPR spectra were obtained at X-band using a Bruker ESP 300 EPR spectrometer in conjunction with a Bruker EN 003 ENDOR/triple interface, a Wavetek 3000-446 radio frequency (rf) synthesizer (a Programmable Test Systems (PTS) rf synthesizer was used as the second source for ST experiments), an EN 370 power amplifier, and an EN 801 ENDOR cavity (estimated *Q* of 800). The Wavetek synthesizer also provided for frequency modulation of the radio frequency output. Temperature control was achieved using an Oxford Instruments continuous flow ESR 900 cryostat with an ITC 4 temperature controller. The impedance of the radio frequency circuit was 50 Ω. ENDOR spectra were acquired at field values corresponding to the crossing point of the first derivative EPR spectrum, and were corrected for baseline nonlinearity by the subtraction of off-resonance scans which were filtered for noise (standard Bruker software) to avoid reducing the spectrum signal to noise ratio. Acquisition conditions for specific spectra are given in the figure captions. Accuracy of hfc determination was ±0.05 MHz.

RESULTS

Tris-Washed PS2. Illumination of Tris-washed PS2 at 77 K produces a *circa* 1 mT wide isotropic EPR spectrum at $g = 2.0025$ that has been ascribed to a Chl *a* cation radical (Nugent et al., 1982)(Figure 2), which we designate $Chl1^{\bullet+}$. The underlying EPR spectrum of $Y_D^{\bullet}$, the dark stable tyrosine radical, may be greatly reduced by preparing samples at pH 8.8 and allowing them to incubate in the dark for 2 h before freezing to 77 K (in the dark) and subsequent illumination. The ENDOR spectrum of $Chl1^{\bullet+}$ is shown in panels a and b of Figure 3. The ENDOR resonances may be assigned by comparison with previously published spectra of Chl *a* cation radicals ($Chla^{\bullet+}$) in frozen and liquid solutions (Scheer et al., 1977; O'Malley & Babcock, 1984; Käss et al., 1994).

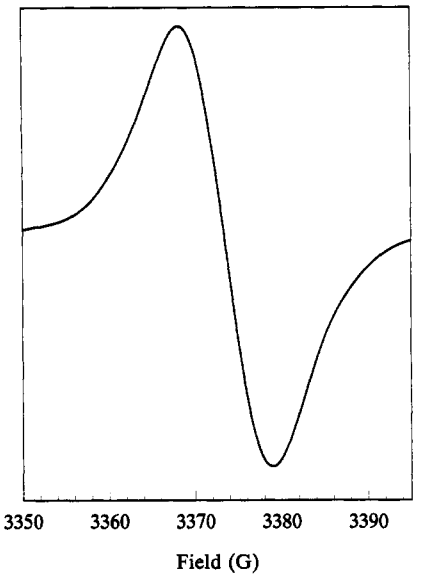

FIGURE 2: EPR spectrum of Chl1$^{\bullet+}$ in Tris-washed PS2 at pH 8.8. The radical was produced by 77 K illumination. Experimental conditions: microwave power, 100 μW; modulation amplitude, 1.2 G; modulation frequency, 12.5 kHz; temperature, 120 K; sum of 2 scans, recorded in the ENDOR cavity.

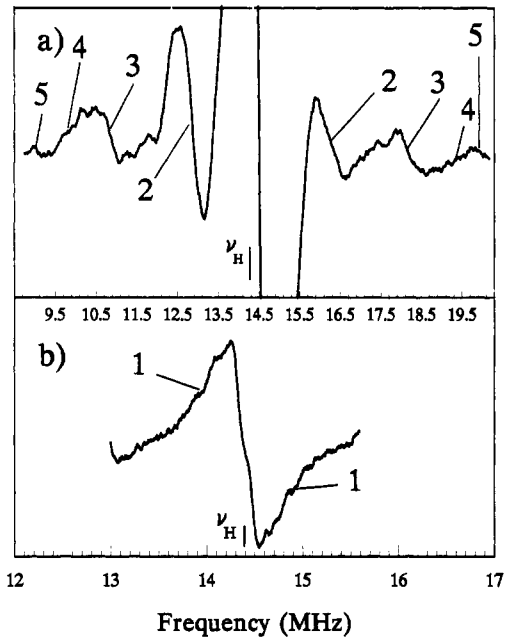

FIGURE 3: ENDOR spectra of Chl1$^{\bullet+}$ at 120 K showing (a) a broad sweep and (b) a matrix region at higher resolution. Numbers refer to resonances assigned in Table 1. Experimental conditions: microwave power 4.9 mW; rf power 50 W; rf modulation depth, (a) 158 and (b) 35 kHz; scan time, 84 s; time constant, 655 ms; sum of 120 scans.

Assignments in these *in vitro* studies were obtained through specific deuteration and theoretical calculations. The most prominent features in chlorophyll radical powder ENDOR spectra arise from rotating methyl groups (Hyde et al., 1968). These occur at positions 1, 3, and 5 in Chl *a* (Figure 1). The ENDOR resonances of such methyl groups are relatively narrow and either isotropic or very weakly axial. This is because for these protons the hyperfine interaction occurs principally through hyperconjugation (i.e., orbital overlap) between the p orbital on the α-carbon (which forms part of the π orbital system containing the unpaired electron) and the methyl protons, which is an isotropic interaction (Fessenden & Schuler 1963). Features 2 and 3 in Figure 3a therefore have the qualities expected of methyl group resonances. Feature 2 corresponds to a hyperfine coupling of 3.6 MHz which is comparable to the average hyperfine coupling reported for the 1 and 3 methyl groups of Chl$a^{\bullet+}$ *in vitro* at 3.2 MHz (Scheer et al., 1977; O'Malley & Babcock, 1984). Feature 3 corresponds to a hyperfine coupling of 7.3 MHz which is very similar to the reported hyperfine coupling of the methyl group at position 5 for Chl$a^{\bullet+}$ *in vitro* [7.56 MHz, Scheer et al. (1977); 7.3 MHz, O'Malley and Babcock (1984)]. The weak feature 1, Figure 3b, corresponds to a hyperfine coupling of 0.9 MHz. Such weak couplings have been previously assigned to the methine protons of Chl$a^{\bullet+}$ *in vitro* (Scheer et al., 1977; O'Malley & Babcock, 1984), although here, because of the possibility of coupling to protons from the surrounding matrix, this assignment must be considered tentative. The largest proton hyperfine couplings observed for Chl$a^{\bullet+}$ *in vitro* arise from the protons at positions 7 and 8 on ring IV (Scheer et al., 1977; Huber et al., 1986; Käss et al., 1994). Although these protons are β to the π system and give rise to sharp resonances in liquid solution, in frozen solution their inequivalence and immobility lead to resonance broadening [for an example of this effect, see Figure 4 in Rautter et al. (1992)]. Feature 4, a hyperfine coupling of 8.2 MHz, has been assigned previously in Chl$a^{\bullet+}$ *in vitro* (O'Malley & Babcock, 1984) as part of a broad resonance arising from the β-protons at positions 7 and 8. A value of 8.0 MHz was reported for this coupling *in vitro* (O'Malley & Babcock, 1984). However, recent studies suggest that this feature arises from the resolved $A_{\|}$ component of methyl 5 (Käss et al., 1994). The resolution of methyl group hyperfine tensors as weakly axial systems is observed, for example, in flavin radicals (Kurreck et al., 1984, 1988). Since the axial splitting increases with A_{iso}, the smaller methyl group couplings are not expected to show such resolved splitting. The 7 and 8 β-protons have also been reported to give rise to weak features with hyperfine couplings of 10–11 MHz (Scheer et al., 1977; Käss et al., 1994). These properties seem consistent with the assignment of feature 5 (Figure 3a) to the 7 and 8 β-protons, with a hyperfine coupling of 10.8 MHz.

The assignments presented above suggest that feature 2 should be resolvable into at least two components, corresponding to the two resonances of methyl groups 1 and 3. This could be achieved by reducing the FM modulation depth of the radio frequency radiation, but at the cost of a reduced signal to noise ratio. Therefore, we have chosen to use ST resonance in order to offset the loss of signal at lower modulation depths. The ST methodology, first proposed by Freed (Freed, 1969) and realized experimentally by Dinse, Biehl, and Möbius (Dinse et al., 1974), uses two rf fields which sweep symmetrically about the nuclear Larmor frequency and thus saturate both transitions arising from each hyperfine coupling simultaneously [see also Möbius and Biehl (1979) and Kurreck et al. (1988)]. This gives rise to a more efficient relaxation bypass than in ENDOR and hence greater resonance intensity. Since both nuclear transitions are swept simultaneously, the ST spectrum contains only one resonance per hyperfine coupling and has the appearance of a "half-ENDOR" spectrum. ST spectra of Chl1$^{\bullet+}$ are shown in Figure 4. Spectrum a in Figure 4 was obtained at 158 kHz modulation depth (as used for the ENDOR spectra) and shows the same features as the ENDOR spectrum in Figure 3a (feature 1 is not visible since our spectrometer does not allow for ST frequencies below 1 MHz). Spectrum b in Figure 4, acquired with a modulation depth of 70 kHz, shows a number of features observed in each sample. Feature 2 is split into two major components, features 2b and 2c. A shoulder is also visible to low frequency, feature 2a. Studies of chlorophyll and related

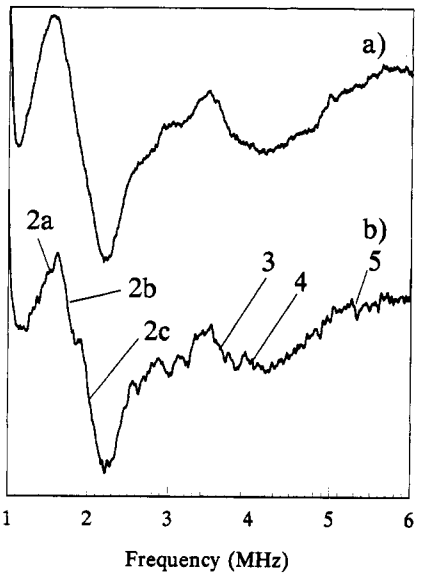

FIGURE 4: ST spectra of Chl1$^{\bullet+}$ at 120 K using (a) 158- and (b) 70-kHz rf modulation depth. Numbers refer to resonances assigned in Table 1. Further experimental conditions: microwave power, 4.9 mW; rf power, 160 W (total over both channels); scan time, 84 s; time constant, 655 ms; sum of 120 scans.

Table 1: Collected Hyperfine Coupling Constants and Assignments for Chlorophyll *a* Radical Cations *in Vivo*

	hyperfine coupling (MHz)				
feature	Chl1$^{\bullet+}$	Chl2$^{\bullet+}$	P680$^{\bullet+}$	P700$^{\bullet+}$	assignment
1	0.9		0.9	0.9	methine
2a	2.8	2.2	2.2	1.8	4-β-CH_2
2b	3.4	2.4	2.8	2.6	1-methyl
2c	4.1	3.2	3.2	3.4	3-methyl
3	7.3	7.7	6.0	5.3	5-methyl $A_\perp$
4	8.2	9.4	7.5	6.3	5-methyl $A_\parallel$
A_{iso}	7.6	8.3	6.5	5.6	5-methyl
5	10.8		8.1	7.2	7,8-β-H

cation radicals *in vitro* suggest that methyl 1 always has a smaller hyperfine coupling constant than methyl 3 (Scheer et al., 1977). Therefore, we assign feature 2b to methyl 1 and 2c to methyl 3. The broader shoulder of feature 2a we assign to the β-methylene protons at position 4. Table 1 shows the Chl1$^{\bullet+}$ hyperfine coupling constants.

PS2 Reaction Centers. Continuous illumination of reaction centers in the presence of the artificial electron acceptor silicomolybdate at low temperatures (in this case 15 K) produces an isotropic EPR spectrum with a line width of 0.76 mT at $g = 2.0025$ (Figure 5b). This species decays rapidly in the dark. During illumination a 1-mT line width dark stable isotropic ($g = 2.0025$) species slowly arises at the expense of the original narrow signal (Figure 5c). The 0.76-mT-wide spectrum has been assigned to the cation radical of the primary donor of PS2, P680$^{\bullet+}$ (Nugent et al., 1989). The narrow width of this spectrum, relative to that of Chl*a*$^{\bullet+}$, is suggestive of a chlorophyll dimer by analogy with the EPR properties of the primary donor of *R. sphaeroides*, P870 (Norris et al., 1971). The dark stable spectrum has a line width (1 mT) consistent with a monomeric Chl *a* cation radical. This species we designate Chl2$^{\bullet+}$.

ENDOR and ST spectra of P680$^{\bullet+}$ are shown in Figure 6. The resonance numbering system of Figures 3 and 4 has been maintained to simplify comparison. Note that Figure 6d shows the ENDOR spectrum of Chl2$^{\bullet+}$ obtained under the same conditions as those in Figure 6a–c. Only a weak matrix signal is observed; thus the P680$^{\bullet+}$ spectra are free of contamination with contributions from Chl2$^{\bullet+}$, outside the matrix region,

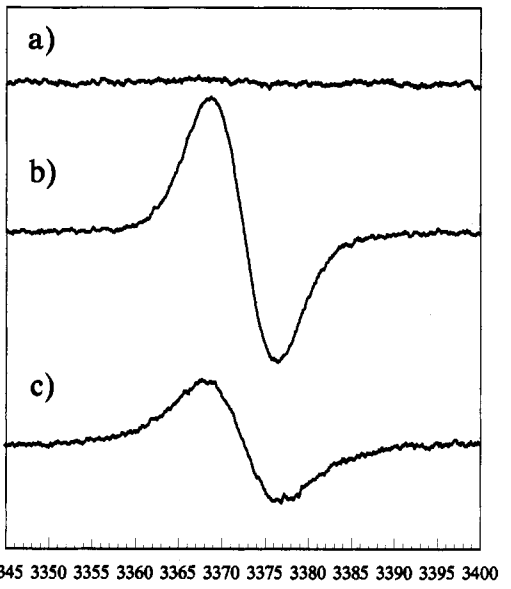

FIGURE 5: EPR spectra of PS2 reaction centers at 15 K (a) in the dark, (b) under continuous illumination (P680$^{\bullet+}$), and (c) in the dark after having been illuminated for 3 h (Chl2$^{\bullet+}$). Experimental conditions: microwave power, 100 μW; modulation amplitude, 1.2 G; modulation frequency, 12.5 kHz; scan time, 84 s; time constant, 327 ms; sum of 4 scans. Spectra were obtained using the ENDOR cavity.

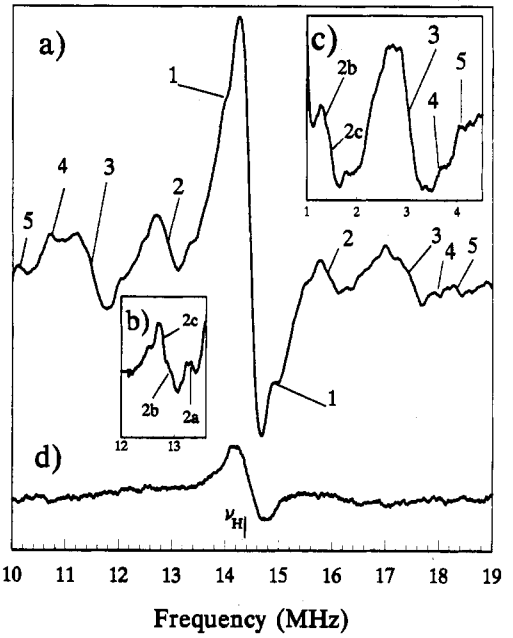

FIGURE 6: ENDOR and ST spectra of P680$^{\bullet+}$ (a–c) and Chl2$^{\bullet+}$ (d) at 15 K. (a) P680$^{\bullet+}$ broad sweep ENDOR; rf modulation depth, 158 kHz. (b) Section of the P680$^{\bullet+}$ ENDOR spectrum; rf modulation depth, 100 kHz. (c) ST spectrum of P680$^{\bullet+}$; rf modulation depth, 100 kHz. (d) Chl2$^{\bullet+}$ broad-sweep ENDOR; rf modulation depth, 158 kHz. Numbers refer to resonances assigned in Table 1. Further conditions: microwave power, 4.9 mW; rf power, 80 W (ENDOR) or 125 W (ST); scan time, 84 s; time constant, 655 ms; 120 scans.

under these conditions. Such temperature dependence suggests that P680$^{\bullet+}$ has shorter electron and nuclear spin relaxation times than Chl2$^{\bullet+}$. This could arise from differences in the dipolar interactions (both electron–electron and electron–nuclear) between the chlorophyll radicals and the paramagnetic cytochrome b_{559}, implying that P680 is closer to b_{559} than Chl2. While no previously published Chl*a*$^{\bullet+}$ spectrum exhibits the same hyperfine couplings as P680$^{\bullet+}$, the pattern of resonances is very similar to that of Chl*a*$^{\bullet+}$ but

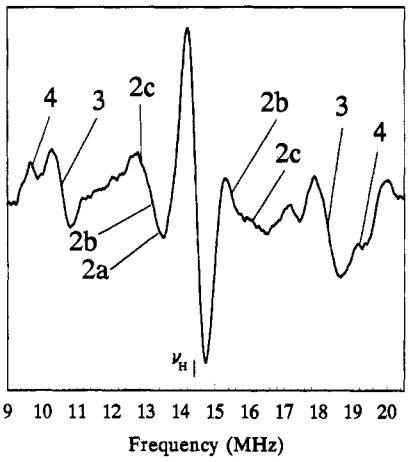

FIGURE 7: ENDOR spectrum of Chl2$^{\bullet+}$ at 120 K. Numbers refer to resonances assigned in Table 1. Experimental conditions: microwave power, 4.9 mW; rf power, 50 W; rf modulation depth, 225 kHz; scan time, 84 s; time constant, 1310 ms; 100 scans.

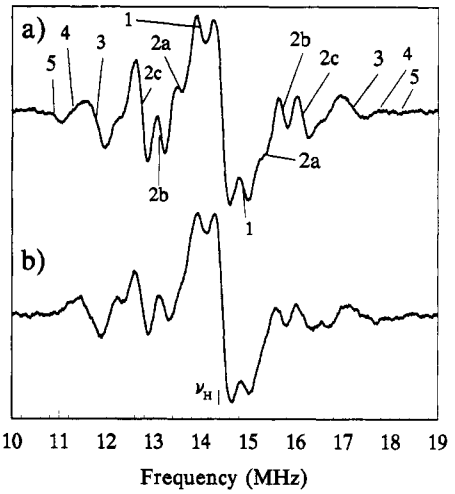

FIGURE 8: ENDOR spectra of P700$^{\bullet+}$ at 10 K in (a) spinach PS1 particles and (b) *Synechocystis* PCC 6803 membranes. Numbers refer to resonances assigned in Table 1. Experimental conditions: microwave power, 6.3 mW; rf power, 63 W; rf modulation depth, 100 kHz; scan time, 84 s; time constant, 655 ms; 80 scans.

with a reduced range of hyperfine couplings. The assignment scheme of Chl1$^{\bullet+}$ is adopted for this species (Table 1). This is consistent with the properties of chlorin cation radicals *in vitro* in which, despite changes in the hyperfine couplings, the ordering from smallest to largest coupling is maintained as methine, methyl 1, methyl 3, methyl 5, and methyl 7/8 β-protons (Scheer et al., 1977). The broad matrix feature around the Larmor frequency precludes the observation of couplings smaller than 1.2 MHz, and the assignment of the methine coupling is tentative.

The ENDOR spectrum of Chl2$^{\bullet+}$ can be obtained at 120 K in the dark, but the spectrum appears to be unstable, and during long periods of scan averaging it decays with time (tens of minutes) to a combined spectrum arising from a mixture of species. A pure species is, however, generated immediately after the light is turned off, and the spectrum of this species may be obtained by summing the first few scans arising from several freshly illuminated samples. While the low signal to noise ratio obtainable from such a procedure precludes the use of small modulation depths, we have been able to acquire the ENDOR spectrum of the first species formed, Chl2$^{\bullet+}$ (Figure 7). Again we have maintained our original resonance numbering scheme. The low resolution of this spectrum does not allow for the separation of the individual components of feature 2, but the distorted line shape is consistent with its multicomponent nature, and this allows for the estimation of the separate hyperfine couplings of methyl groups 1 and 3. Features 1 (methine protons) and 5 (7 and 8 β-protons) are also not observed under these conditions. The use of ST does not allow the rf modulation depth to be reduced to a point where the available resolution is significantly increased for this radical. The resonance visible between features 2 and 3 on the high-frequency side of the Larmor frequency is as yet unassigned. This resonance is observed in many chlorophyll ENDOR spectra (normally as a shoulder, as it is to low field of the Larmor frequency in Figure 7) including those in this paper and previously published spectra of P700$^{\bullet+}$ and Chl*a*$^{\bullet+}$ (O'Malley & Babcock, 1984), and is not a special feature of Chl2$^{\bullet+}$. The clean definition of the resonances (with the exception of 2 for reasons mentioned above) is consistent with the spectrum arising from a single species. The hyperfine coupling constants obtained for Chl2$^{\bullet+}$ are presented in Table 1. Despite the assignment of Chl2$^{\bullet+}$ as a Chl *a* radical cation, the hyperfine couplings differ from those of Chl*a*$^{\bullet+}$ *in vitro* and Chl1$^{\bullet+}$. Chl2$^{\bullet+}$ shows smaller couplings to methyl groups 1 and 3 and larger couplings to the methyl 5 group. The significance of such differences is discussed below.

Table 2: ENDOR Observable Electron Spin Densities (ρ_o) at Carbon Atoms of Chlorophyll *a* Cation Radicals *in Vivo*, calculated from the Data of Table 1

carbon atom	Chl1$^{\bullet+}$	Chl2$^{\bullet+}$	P680$^{\bullet+}$	P700$^{\bullet+}$
1	0.032	0.023	0.026	0.024
3	0.039	0.030	0.030	0.032
5	0.072	0.079	0.062	0.053
$\Sigma \rho_o$	0.143	0.132	0.118	0.109

ENDOR Spectrum of P700$^{\bullet+}$. The only Chl*a*$^{\bullet+}$ that has been previously studied *in vivo* is P700$^{\bullet+}$ (Norris et al., 1974; Hoff, 1979; O'Malley & Babcock, 1984), the oxidized primary donor of PS1. We have measured the ENDOR spectrum of this radical in two different preparations (Figure 8), purified PS1 from spinach (*Spinacea oleracea*) and *Synechocystis* PCC 6803 membranes, for comparison with the PS2 data presented above. Slight differences in some of the hyperfine couplings were observed between the two PS1 preparations. These may arise from the different preparation methods employed or may reflect species-dependent divergence in the environment of P700$^{\bullet+}$. The hyperfine coupling constants as presented in Table 1 are in good agreement with those obtained previously.

Electron Spin Density Estimations. The electron spin density at the ring carbon to which a rotating methyl group is attached is given by the McConnell relation (McConnell 1956): $A = Q\rho$, where Q has the value 106 MHz (Scheer et al., 1977), ρ is the electron spin density at the attached carbon atom, and A is the isotropic hyperfine coupling constant. The electron spin densities calculated from the hyperfine coupling data of Table 1 for P680$^{\bullet+}$, Chl1$^{\bullet+}$, Chl2$^{\bullet+}$, and P700$^{\bullet+}$ are given in Table 2. For the assignment scheme, the methyl 5 A_{iso} must be calculated as $(2A_\perp + A_\parallel)/3$, where $A_\perp$ is feature 3 and $A_\parallel$ is feature 4. Data for methine carbons are not given since the assignment of these resonances is uncertain. Electron spin densities for carbons 4, 7, and 8 are also omitted, although we have determined hyperfine coupling constants for the β-methylene group at position 4 and the 7 and 8 β-protons. The hyperfine coupling constants of such nonrotating β-protons are given by the Heller–McConnell equation (Heller & McConnell, 1960), $A_{iso} = (B_0 + B_2 \cos^2 \Theta)\rho$, where B_0 and B_2 are constants and Θ is the dihedral angle between the C–H bond to the proton and the p_z orbital of the π system.

Since we cannot determine Θ for such β-protons, the electron spin density, ρ, also cannot be determined. Table 2 also lists the sum of the electron spin density which is measurable using ENDOR, $\sum \rho_o$ (sum observable spin density) for each radical (errors due to the omission of the methine carbons are negligible since such carbon atoms have low ρ).

DISCUSSION

Since the hyperfine coupling constants of Chl1$^{\bullet+}$ have values close to those of Chl*a*$^{\bullet+}$ *in vitro* (Käss et al., 1994; Scheer et al., 1977; O'Malley et al., 1984), this radical may be taken as a standard for protein-associated Chl*a*$^{\bullet+}$ *in vivo*. The ratio $\sum \rho_o$:$\sum \rho_o$(Chl1$^{\bullet+}$) for each radical should give an indication of any reduction in its observable, and hence its total, electron spin density. Any such decrease would require that spin density is asymmetric and partly relocated to another molecule which is not observed in the ENDOR experiment. Such a molecule could be one-half of a chlorophyll dimer of which the ENDOR-observable molecule constitutes the other half. Note that, as mentioned above, the broad matrix features of the chlorophyll radicals preclude the ready observation of couplings smaller than *circa* 1.2 MHz. Furthermore, the resonances arising from such small couplings may have line widths greater than their separation, preventing their resolution. Thus a chlorophyll radical with a low $\sum \rho_o$ could be concealed beneath the matrix feature. The $\sum \rho_o$:$\sum \rho_o$(Chl1$^{\bullet+}$) ratios for P680$^{\bullet+}$, Chl2$^{\bullet+}$, and P700$^{\bullet+}$ are 0.82, 0.91, and 0.75 (spinach) (errors in these ratios are estimated at ±0.03 from the uncertainty in the ENDOR measurements). From the apparent reduction in spin density values, it appears that P680$^{\bullet+}$ may be a Chl *a* pair with the unpaired electron spin density distributed in a ratio of *circa* 5:1, Chl2$^{\bullet+}$ is a Chl *a* monomer, and P700$^{\bullet+}$ is a Chl *a* pair with the unpaired electron spin density distributed in a ratio of *circa* 3:1. For both P680$^{\bullet+}$ and P700$^{\bullet+}$ the Chl *a* molecule with the lower electron spin density presumably does not give rise to observable ENDOR because it is hidden in the matrix region, and therefore we cannot rigorously discount the possibility that these species are modified chlorophyll monomers (see later discussion). Electron spin echo envelope modulation analysis of ^{14}N hyperfine and quadrupole couplings in P700$^{\bullet+}$ suggests that the spin density distribution ratio over the two halves of the Chl *a* pair is 3:1 or 4:1 (Davis et al., 1993).

The reduction of the EPR line width of P870$^{\bullet+}$, relative to bacteriochlorophyll *a*$^{\bullet+}$, by a factor of $2^{-1/2}$ was originally taken as evidence for a symmetrical dimeric structure for the primary donor in *R. sphaeroides* (Norris et al., 1971). Recent ENDOR studies of reaction center single crystals have now shown a 2:1 distribution of electron spin density over the two bacteriochlorophyll molecules with most spin on the L half (Lendzian et al., 1990, 1993). The EPR line width reduction factor of P680$^{\bullet+}$, relative to Chl*a*$^{\bullet+}$, is very similar to that of P870$^{\bullet+}$ (i.e., $2^{-1/2}$). However, for inhomogeneously broadened lines, the line width is most sensitive to variations in the largest hyperfine coupling constants. For chlorophylls the largest coupling constants are those of the β-protons at positions 7 and 8 (Scheer et al., 1977). Therefore, the EPR line width tends to be more sensitive to the electron spin density at chlorophyll ring IV than to the total distribution. A further complication to the interpretation of EPR line widths is the effect of **g** anisotropy. Studies of chlorophyll radicals employing high-frequency EPR [Klette et al. (1993) at 95 GHz and Gulin et al. (1992) at 135 GHz] have allowed for accurate determination of the **g** tensor anisotropy of chlorophyll dimers and have revealed an increase in anisotropy, relative to monomers, which is dependent on the dimer geometry. Therefore, the interpretation of EPR line widths for the photosynthetic primary donor cation radicals in terms of structure is not as simple as that originally advanced.

A possible solution to this problem is to measure the electron spin density distribution over the primary donor using ENDOR. Unfortunately, it has not proved possible to observe ENDOR resonances for every proton in a chlorophyll molecule even *in vitro*, in solution (Kurreck et al., 1988). Furthermore, many carbon atoms in chlorophyll molecules lack attached protons or β-protons and would require the use of ^{13}C ENDOR, in solution, to reduce hyperfine anisotropy broadening. This is a technique which is rarely applied to biological systems because of the need to enrich in the ^{13}C isotope (the natural abundance is *circa* 1.1%) and the requirement for rapid molecular tumbling in solution to average the hyperfine anisotropy. ENDOR can, however, provide an estimate of the electron spin density distribution through the measurement of methyl group and some β-proton hyperfine couplings. Since these protons occupy the same positions in all Chl *a* radicals, they can be used comparatively to assess differences in electron spin density between individual radical species.

The nature of P680, whether a Chl *a* monomer or two closely spaced Chl *a* molecules, has been a subject of controversy for some time. The high degree of sequence homology between the D1/D2 proteins of PS2 and the L/M proteins of the bacterial reaction centers argues for a "bacterial" arrangement with a closely associated chlorophyll pair (Svensson et al., 1990; Ruffle et al., 1992). Spectroscopic studies have supported both options. Zero field splitting parameters measured through EPR studies of the P680 triplet state support a monomeric structure with the possibility that P680 is analogous to the accessory chlorophylls in bacterial reaction centers (van Mieghem et al., 1991). Low-temperature time-resolved (Durrant et al., 1990; van Kan et al., 1990) and steady state (Braun et al., 1990; Kwa et al., 1992; Otte et al., 1992) optical techniques suggest that the ground state of P680 is dimeric with a weaker exciton splitting (85–100 cm^{-1}) than the bacterial primary donors (600–1500 cm^{-1}; Knapp et al., 1985; Scherer & Fischer, 1987), but that formation of the triplet and radical cation states involves only one-half of the dimer. The weak exciton splitting and localization of the paramagnetic states could be due to an increased separation or a different relative orientation of the constituent monomers of the pair relative to their bacterial analogues (Tetenkin et al., 1989). A similar conclusion was reached in a recent study using picosecond transient absorption spectroscopy which also indicated that P680 was a dimer (Schelvis et al., 1994). Hole-burning studies of the excited singlet state (^{1}P680*) suggest a P680 dimer, but again one that differs signficantly in its geometry and/or excited-state electronic distribution from ^{1}P870* or ^{1}P960* (Jankowiak et al., 1989; Tang et al., 1990). Absorption detected magnetic resonance (ADMR) of the triplet state originally suggested a dimeric structure for P680 (den Blanken et al., 1983), but more recent data using improved protein isolation procedures favors a monomer with little or no exciton splitting (van der Vos et al., 1992). Vibrational spectroscopy has also been employed. The bleaching of a single keto carbonyl stretching band is observed on triplet formation in resonance Raman spectroscopy at low temperature (15 K), suggesting that the triplet state is localized on one chlorophyll (Moenne-Loccoz et al., 1990). However, a Fourier transform infrared spectroscopic study of the same phenomenon but at higher temperatures (80 K) shows bleaching of two carbonyl bands with different intensities corresponding to an asymmetric dimer with an 86:14 triplet state distribution between the two dimer components (Noguchi

et al., 1993). Previous EPR studies of $P680^{\bullet+}$ have interpreted the reduced line width as indicating a modified monomer or a dimeric structure (van Gorkom et al., 1974; Davis et al., 1979; Nugent et al., 1989). The consensus from all of these results appears to favor a monomer or two weakly interacting molecules (depending on the strength of the interaction, these may not be distinguishable) in the ground state (and possibly $^1P680^*$) with a temperature-dependent distribution of the triplet state.

The ENDOR data presented here for $P680^{\bullet+}$ implies that this state has a high degree of monomeric character but probably involves two weakly interacting chlorophyll molecules. The spin density distribution we calculate for $P680^{\bullet+}$ with 82% of the unpaired electron spin on one-half of the pair (at 15 K) is essentially the same as that suggested for the triplet state distribution at 80 K by Noguchi et al. (1993). Since the weak interaction between the two molecules is not consistent with the concept that the region of PS2 around P680 resembles the analogous region of the bacterial reaction center, the unusual orientation of one chlorophyll bearing the P680 triplet at 4.4 K suggested by EPR (van Mieghem et al., 1991) does not preclude this chlorophyll from forming part of the primary donor of PS2. The concentration of electron spin density on one Chl *a* of $P680^{\bullet+}$ requires that either the relative orientation or the separation of the pair is different from that of the bacterial primary donors. Such an arrangement may be made possible by the two conserved prolines (D1-279, D2-276) in the PS2 structure which are predicted to lie within helix V, which bears the primary donor histidine ligands (Ruffle et al., 1992). Proline residues in protein helices act as hinges and are associated with helix bending. This would allow for a larger cavity about the primary donor than is observed in bacterial reaction centers that lack these residues. However, it is unlikely that even this larger pocket would accommodate the proposed structure of Noguchi et al. (1993), with one chlorophyll tilted at a steep angle to the other. It is important to note that the ENDOR data presented here refers to the radical cation state $P680^{\bullet+}$; the electronic structures of the ground, excited singlet ($^1P680^*$), and triplet states could differ from this. Furthermore, the high $\sum \rho_o$ and the relatively small decreases in the hyperfine coupling constants of $P680^{\bullet+}$ relative to those of $Chla^{\bullet+}$ *in vitro* could arise from environmental effects. These could involve ring IV of a Chl *a* monomer, although reductions in methyl group couplings of this magnitude appear to require covalent modification of Chl *a* (Scheer et al., 1977; Davis et al., 1979). The possibility of admixing the first excited state into the ground state in chlorin radical cations has been advanced previously as a cause of reduced proton hyperfine couplings observed in ENDOR spectra of $P700^{\bullet+}$ and $P870^{\bullet+}$ (O'Malley & Babcock, 1984). While we cannot exclude this mechanism as a contributory factor to the reduced hyperfine couplings in $P680^{\bullet+}$, subsequent investigations of the electronic structure of $P700^{\bullet+}$ and $P870^{\bullet+}$ (and $P960^{\bullet+}$) have shown decreased nitrogen hyperfine coupling in these species (Davis et al., 1993; Lendzian et al., 1993), whereas orbital admixing is predicted to give an increase in these couplings (O'Malley & Babcock, 1984; Petke et al., 1980).

Much less information is available on the monomeric chlorophylls which give rise to radicals $Chl1^{\bullet+}$ and $Chl2^{\bullet+}$. $Chl1^{\bullet+}$ has been identified in EPR spectra (Nugent et al., 1982; Miller & Brudvig, 1991) and has been suggested to play a role in photoinhibition (Thompson & Brudvig, 1988). $Chl2^{\bullet+}$ has also been observed in EPR spectra (Nugent et al., 1989), but the distinction between $Chl2^{\bullet+}$ and $Chl1^{\bullet+}$ has not been possible because of the similarity of their EPR spectra. A chlorophyll molecule which is stably oxidized on room temperature illumination of PS2 reaction centers has been detected in optical spectra and termed C670 (Telfer et al., 1990a,b). This may be the source of $Chl2^{\bullet+}$. Owing to the differences between the preparations that yield $Chl1^{\bullet+}$ and $Chl2^{\bullet+}$, it is possible that they arise from different forms of the same chlorophyll molecule.

$Chl1^{\bullet+}$ has hyperfine coupling constants very similar to those of $Chla^{\bullet+}$ *in vitro* in 5:1 CH_2Cl_2:tetrahydrofuran (O'Malley & Babcock 1984). This suggests that $Chl1^{\bullet+}$ has one axial magnesium ligand (probably a histidine) and a hydrophobic environment (Hägele et al., 1978a,b). Relative to $Chl1^{\bullet+}$, $Chl2^{\bullet+}$ has a higher electron spin density at carbon 5 and a lower spin density at carbons 1 and 3 (Table 2). Such a trend has been observed in $Chla^{\bullet+}$ in non-coordinating solvents (pure CH_2Cl_2) (Davis et al., 1979) and suggests that $Chl2^{\bullet+}$ may not have axial coordination. This is of interest since the histidines that coordinate the accessory chlorophylls in the bacterial reaction center are not conserved in PS2 (Svensson et al., 1990; Ruffle et al., 1992) and may not be necessary for the binding of these chlorophylls (Coleman & Youvan, 1990). The presence of a chlorophyll so close to P680 would suggest more rapid oxidation kinetics than observed for $Chl1^{\bullet+}$. We have previously suggested from our model of PS2 (Ruffle et al., 1992) that His 118 in D1 and D2, located on the periphery of the complex, could provide a chlorophyll ligand. This would be an appropriate position for an accessory chlorophyll with the properties of $Chl1^{\bullet+}$.

In conclusion, ENDOR spectroscopy has identified three Chl *a* cation radicals in PS2. Two arise from isolated Chl *a* monomers, one of which may lack amino acid coordination. The third is associated with the presumptive donor, P680, which is suggested to be a Chl *a* pair with a *circa* 5:1 spin density ratio over its constituent halves. While some suggestions as to the geometry of P680 can be made from the ENDOR data, detailed characterization of P680 awaits the results of X-ray crystallographic studies.

REFERENCES

Allen, J. P., Feher, G., Yeates, T. O., Rees, D. C., Deisenhofer, J., Michel, H., & Huber, R. (1986) *Proc. Natl. Acad. Sci. U.S.A. 83*, 8589.

Barber, J., Chapman, D. J., & Telfer, A. (1987) *FEBS Lett. 220*, 67.

Berthold, D. A., Babcock, G. T., & Yocum, C. F. (1981) *FEBS Lett. 134*, 231.

Biggins, J., & Mathis, P. (1988) *Biochemistry 27*, 1494.

Blankenship, R. E., & Prince, R. C. (1985) *Trends Biochem. Sci. 10*, 382.

Braun, P., Greenberg, B. M., & Scherz, A. (1990) *Biochemistry 29*, 10376.

Chandrashekar, T. K., O'Malley, P. J., Rodriguez, I., & Babcock, G. T. (1986) *Photosynth. Res. 10*, 423.

Clayton, B. J., & Clayton, R. K. (1978) *Biochim. Biophys. Acta 501*, 470.

Coleman, W. J., & Youvan, D. C. (1990) *Annu. Rev. Biophys. Biophys. Chem. 19*, 333.

Davis, I. H., Heathcote, P., MacLachlan, D. J., & Evans, M. C. W. (1993) *Biochim. Biophys. Acta 1143*, 183.

Davis, M. S., Foreman, A., & Fajer, J. (1979) *Proc. Natl. Acad. Sci. U.S.A. 76*, 4170.

Deisenhofer, J., & Norris, J. R. Eds. (1993) *The Photosynthetic Reaction Center*, Vols. 1 and 2, Academic Press, San Diego.

Deisenhofer, J., Epp, O., Miki, R., Huber, R., & Michel, H. (1985) *Nature (London) 318*, 618.

Demetriou, C. (1990) Ph.D. Thesis, University College London.

den Blanken, H. J., Hoff, A. J., Jongenelis, A. P. J. M., & Diner, B. A. (1983) *FEBS Lett. 157*, 21.

Dinse, K. P., Biehl, R., & Möbius, K. (1974) *J. Chem. Phys. 61*, 4335.
Durrant, J. R., Giorgi, L. B., Barber, J., Klug, D. R., & Porter, G. (1990) *Biochim. Biophys. Acta 1017*, 167.
Evans, M. C. W., & Nugent, J. H. A. (1993) in *The Photosynthetic Reaction Center* (Deisenhofer, J., & Norris, J. R., Eds.) Vol. 1, p 391, Academic Press, San Diego.
Feher, G., Hoff, A. J., Isaacson, R. A., & Ackerson, L. C. (1975) *Ann. N.Y. Acad. Sci. 244*, 239.
Feher, G., Isaacson, R. A., Okamura, M. Y., & Lubitz, W. (1988) in *The Photosynthetic Bacterial Reaction Center: Structure and Dynamics* (Breton, J., & Verméglio, A., Eds.) p 229, Plenum Press, New York.
Fessenden, R. W., & Schuler, R. H. (1963) *J. Phys. Chem. 39*, 2147.
Ford, R. C., & Evans, M. C. W. (1983) *FEBS Lett. 160*, 159.
Freed, J. H. (1969) *J. Chem. Phys. 50*, 2271.
Gulin, V. I., Dikanov, S. A., Tsvetskov, Yu. D., Evelo, R. G., & Hoff, A. J. (1992) *Pure Appl. Chem. 64*, 903.
Hägele, W., Schmid, D., & Wolf, H. C. (1978a) *Z. Naturforsch. A33*, 83.
Hägele, W., Schmid, D., & Wolf, H. C. (1978b) *Z. Naturforsch. A33*, 94.
Heller, H. C., & McConnell, H. M. (1960) *J. Chem. Phys. 32*, 1535.
Hoff, A. J. (1979) *Phys. Rep. 54*, 75.
Hoff, A. J. (1993) in *The Photosynthetic Reaction Center* (Deisenhofer, J., & Norris, J. R., Eds.) Vol. 2, p 331, Academic Press, San Diego.
Huber, M., Lendzian, F., Lubitz, W., Tränkle, E., Möbius, K., & Wasielewski, M. R. (1986) *Chem. Phys. Lett. 132*, 467.
Hyde, J. S., Rist, G. H., & Eriksson, L. E. G. (1968) *J. Phys. Chem. 72*, 4269.
Jankowiak, R., Tang, D., Small, G. J., & Seibert, M. (1989) *J. Phys. Chem. 93*, 1649.
Käss, H., Rautter, J., Zweygart, W., Struck, A., Scheer, H., & Lubitz, W. (1994) *J. Phys. Chem. 98*, 354.
Klette, R., Törring, J. T., Plato, M., Möbius, K., Bönigk, B., & Lubitz, W. (1993) *J. Phys. Chem. 97*, 2015.
Knapp, E. W., Fischer, S. F., Zinth, W., Sander, M., Kaiser, W., Deisenhofer, J., & Michel, H. (1985) *Proc. Natl. Acad. Sci. U.S.A. 82*, 8463.
Kurreck, H., Bock, M., Bretz, N., Elsner, M., Kraus, H., Lubitz, W., Müller, F., Geissler, J., & Kroneck, P. M. H. (1984) *J. Am. Chem. Soc. 106*, 737.
Kurreck, H., Kirste, B., & Lubitz, W. (1988) *Electron Nuclear Double Resonance Spectroscopy of Radicals in Solution: Application to Organic and Biological Chemistry*, VCH Publishers, Weinheim, Germany.
Kwa, S. L. S., Newell, W. R., van Grondelle, R., & Dekker, J. P. (1992) *Biochim. Biophys. Acta 1099*, 193.
Lendzian, F., Lubitz, W., Scheer, H., Hoff, A. J., Plato, M., Tränkle, E., & Möbius, K. (1988) *Chem. Phys. Lett. 148*, 377.
Lendzian, F., Endeward, B., Plato, M., Bumann, D., Lubitz, W., & Möbius, K. (1990) in *Reaction Centres of Photosynthetic Bacteria* (Michel-Beyerle, M. E., Ed.) Springer Series in Biophysics, Vol. 6, p 57, Springer, Berlin.
Lendzian, F., Gessner, C., Bönigk, B., Plato, M., Möbius, K., & Lubitz, W. (1992) in *Research in Photosynthesis* (Murata, N., Ed.) Vol. 1, p 433, Kluwer Academic Publishers, Dordrecht, The Netherlands.
Lendzian, F., Huber, M., Isaacson, R. A., Endeward, B., Plato, M., Bönigk, B., Möbius, K., Lubitz, W., & Feher, G. (1993) *Biochim. Biophys. Acta 1183*, 139.
Lubitz, W., Lendzian, F., Scheer, H., Gottstein, J., Plato, M., & Möbius, K. (1984) *Proc. Natl. Acad. Sci. U.S.A. 81*, 1401–1405.
Lubitz, W., Isaacson, R. A., Okamura, M. Y., Abresch, E. C., Plato, M., & Feher, G. (1989) *Biochim. Biophys. Acta 977*, 227.
McConnell, H. M. (1956) *J. Chem. Phys. 24*, 764.
Miller, A.-F., & Brudvig, G. W. (1991) *Biochim. Biophys. Acta 1056*, 1.
Möbius, K., & Biehl, R. (1979) in *Multiple Electron Resonance Spectroscopy* (Dorio, M. M., & Freed, J. H., Eds.) p 480, Plenum Press, New York.
Moenne-Loccoz, P., Robert, B., & Lutz, M. (1990) in *Current Research in Photosynthesis* (Baltscheffsky, M., Ed.) Vol. I, p 423, Kluwer Academic Publishers, Dordrecht, The Netherlands.
Nanba, O., & Satoh, K. (1987) *Proc. Natl. Acad. Sci. U.S.A. 84*, 109.
Noguchi, T., Inoue, Y., & Satoh, K. (1993) *Biochemistry 32*, 7186.
Norris, J. R., Uphaus, R. A., Crespi, H. L., & Katz, J. J. (1971) *Proc. Natl. Acad. Sci. U.S.A. 76*, 4170.
Norris, J. R., Scheer, H., Druyen, M. E., & Katz, J. J. (1974) *Proc. Natl. Acad. Sci. U.S.A. 71*, 4897.
Norris, J. R., Scheer, H., & Katz, J. J. (1975) *Ann. N.Y. Acad. Sci. 244*, 260.
Nugent, J. H. A., Evans, M. C. W., & Diner, B. A. (1982) *Biochim. Biophys. Acta 682*, 106.
Nugent, J. H. A., Telfer, A., Demetriou, C., & Barber, J. (1989) *FEBS Lett. 255*, 53.
O'Malley, P. J., & Babcock, G. T. (1984) *Proc. Natl. Acad. Sci. U.S.A. 81*, 1098.
O'Malley, P. J., Babcock, G. T., & Prince, R. C. (1984) *Biochim. Biophys. Acta 766*, 283.
Otte, S. C. M., van der Vos, R., & van Gorkom, H. J. (1992) *J. Photochem. Photobiol. B 15*, 5.
Petke, J. D., Maggiora, G. M., Shipman, L. L., & Christoffersen, R. E. (1980) *Photochem. Photobiol. 31*, 243.
Rautter, J., Gessner, C., Lendzian, F., Lubitz, W., Williams, J. C., Murchison, H. A., Wang, S., Woodbury, N. W., & Allen, J. P. (1992) in *The Photosynthetic Bacterial Reaction Centre II* (Breton, J., & Verméglio, A., Eds.) p 99, Plenum Press, New York.
Rigby, S. E. J., Nugent, J. H. A., & O'Malley, P. J. (1994) *Biochemistry 33*, 1734.
Ruffle, S. V., Donnelly, D., Blundell, T. L., & Nugent, J. H. A. (1992) *Photosynth. Res. 34*, 287.
Scheer, H., Katz, J. J., & Norris, J. R. (1977) *J. Am. Chem. Soc. 99*, 1372.
Schelvis, J. P. M., van Noort, P. I., Aartsma, T. J., & van Gorkom, H. J. (1994) *Biochim. Biophys. Acta 1184*, 242.
Scherer, P. O. J., & Fischer, S. F. (1987) *Biochim. Biophys. Acta 891*, 157.
Svensson, B., Vass, I., Cedergren, E., & Styring, S. (1990) *EMBO J. 9*, 2051.
Tang, D., Jankowiak, R., Seibert, M., Yocum, C. F., & Small, G. J. (1990) *J. Phys. Chem. 94*, 6519.
Telfer, A., He, W.-Z., & Barber, J. (1990a) *Biochim. Biophys. Acta 1017*, 143.
Telfer, A., Durrant, J., & Barber, J. (1990b) *Biochim. Biophys. Acta 1018*, 168.
Tetenkin, V. L., Gulyaev, B. A., Seibert, M., & Rubin, A. B. (1989) *FEBS Lett. 250*, 459.
Thompson, L. K., & Brudvig, G. W. (1988) *Biochemistry 27*, 6653.
van der Vos, R., van Leeuwen, P. J., Braun, P., & Hoff, A. J. (1992) *Biochim. Biophys. Acta 1140*, 184.
van Gorkom, H. J., Tamminga, J. J., & Haveman, J. (1974) *Biochim. Biophys. Acta 347*, 417.
van Kan, P. J. M., Otte, S. C. M., Kleinherenbrink, F. A. M., Nieveen, M. C., Aartsma, T. J., & van Gorkom, H. J. (1990) *Biochim. Biophys. Acta 1020*, 146.
van Mieghem, F. J. E., Satoh, K., & Rutherford, A. W. (1991) *Biochim. Biophys. Acta 1058*, 379.
Williams-Smith, D. L., Heathcote, P., Sihra, C. K., & Evans, M. C. W. (1978) *Biochem. J. 170*, 365.